LA-UR-21-26260
Accepted Manuscript

Perovskite oxynitrides as tunable materials for electrocatalytic nitrogen reduction to ammonia

Young, Samuel David
Banerjee, Amitava
Pilania, Ghanshyam
Goldsmith, Bryan R.

Provided by the author(s) and the Los Alamos National Laboratory (2022-04-14).

To be published in: Trends in Chemistry

DOI to publisher's version: 10.1016/j.trechm.2021.07.002

Permalink to record:
http://permalink.lanl.gov/object/view?what=info:lanl-repo/lareport/LA-UR-21-26260

Los Alamos National Laboratory, an affirmative action/equal opportunity employer, is operated by Triad National Security, LLC for the National Nuclear Security Administration of U.S. Department of Energy under contract 89233218CNA000001. By approving this article, the publisher recognizes that the U.S. Government retains nonexclusive, royalty-free license to publish or reproduce the published form of this contribution, or to allow others to do so, for U.S. Government purposes. Los Alamos National Laboratory requests that the publisher identify this article as work performed under the auspices of the U.S. Department of Energy. Los Alamos National Laboratory strongly supports academic freedom and a researcher's right to publish; as an institution, however, the Laboratory does not endorse the viewpoint of a publication or guarantee its technical correctness.

Perovskite Oxynitrides as Tunable Materials for Electrocatalytic Nitrogen Reduction to Ammonia

Samuel D. Young[1,2], Amitava Banerjee[2], Ghanshyam Pilania[2]*, Bryan R. Goldsmith[1]*

1. Department of Chemical Engineering, University of Michigan, 2300 Hayward St., Ann Arbor, MI 48109-2136, USA

2. Los Alamos National Laboratory, P.O. Box 1663, Los Alamos, NM 87545, USA

* Correspondence: gpilania@lanl.gov (G. Pilania); bgoldsm@umich.edu (B.R. Goldsmith)

Abstract

The electrocatalytic nitrogen reduction reaction (ENRR) to ammonia is a potentially sustainable alternative to the Haber-Bosch process, but low Faradaic efficiencies and rates hinder its implementation. Perovskite oxynitrides are a tunable class of materials with unique chemistry for ENRR. Elucidating structure-property-mechanism relations for perovskite oxynitrides will aid ENRR catalyst design.

Keywords: ammonia synthesis, oxynitrides, materials chemistry, electrocatalysis

Ammonia (NH_3) is crucial for the world's economy as a fertilizer feedstock, industrial chemical, and hydrogen storage molecule [1]. The production of NH_3 currently depends on the capital- and energy-intensive Haber-Bosch (HB) process. One attractive HB alternative with lower total CO_2 emissions is the electrocatalytic nitrogen reduction reaction (ENRR, $N_2 + 6\,H^+ + 6\,e^- \rightleftharpoons 2\,NH_3$) [2]. Efficient ENRR would also enable decentralized ammonia production, which is essential to communities without centralized infrastructure.

Platinum group metals (PGMs) are often studied as ENRR catalysts because of their stability under acidic conditions. However, ENRR on PGMs is hindered by (1) low Faradaic efficiencies due to the competing hydrogen evolution reaction (HER) and (2) low turnover frequencies (TOFs) due to the strength of the triple bond in N_2 [1]. Alloys, single atom catalysts, and metal nitrides are currently being explored to improve ENRR activity and selectivity, but no existing material exhibits suitable performance thus far. For example, even a state-of-the-art Fe single-atom catalyst supported on N-doped carbon achieves only 56% Faradaic efficiency and an NH_3 yield of 1.30×10^{-12} mol NH_3 cm^{-2}_{ECSA} s^{-1} [3], far below the U.S. Department of Energy target of 9.3×10^{-7} mol NH_3 cm^{-2}_{ECSA} s^{-1} [2].

Perovskite oxynitrides represent a highly tunable alternative to PGM catalysts, where nitrogen replaces some oxygen anions in a perovskite structure. Perovskite oxynitrides have composition $ABO_{3-x}N_x$, where A and B are cations and $0 < x < 3$. Figure 1a shows a typical $ABON_2$ perovskite oxynitride, with 12-fold-coordinated A-site cations and 6-fold-coordinated B-site cations. Along with O and N anion ordering and composition, the choice of A and B cations with flexible oxidation states creates a large combinatorial space for tuning metal-anion interactions and surface-adsorbate bonds. At least 68 single perovskite oxynitride materials have been synthesized, and many more potentially synthesizable structures have been predicted [4]. Beyond simple metal oxynitrides, the exploration of single, double, and layered perovskite oxynitrides enlarges the design space by several orders of magnitude. This high tunability may allow fine-tuning each reaction step's energetics to optimize ENRR thermodynamics and kinetics [5].

Oxynitrides are likely more effective than transition metal nitrides at adsorbing N_2 and activating its triple bond while mitigating HER, which improves the overall reaction rate and selectivity [2]. Several studies have focused on vanadium oxynitrides (VONs) as model ENRR catalysts. Density functional theory (DFT) studies predict that VON is more active than vanadium nitride (VN) for ENRR. The presence of O anions also inhibits V leaching and increases ENRR selectivity towards NH_3 [6]. X-ray absorption spectroscopy suggests that VON, not VN, is the likely active phase for ENRR and that the active N sites are specifically those next to an O site [7]. The N≡N triple bond can be weakened by transferring electrons to the 2*p* antibonding orbitals or removing electrons from the 2*p* bonding orbitals. Having O anions alongside N in the surface or subsurface regions facilitates electron transfer. Oxygen in the subsurface indirectly modulates the surface transition metal and nitrogen electronic states due to the hybridization of

surface metal *d*-states with N and O *p*-states, shifting the VON *d*-band center closer to the Fermi level than that of VN [6].

Nitrogen reduction to ammonia on metal nitrides and oxynitrides often proceeds via a Mars-van-Krevelen (MvK) mechanism facilitated by surface N vacancies [7,8]. The left portion of Figure 1b shows one possible ENRR mechanism: N_2 adsorbs to heal an N vacancy and then undergoes stepwise hydrogenation via concerted proton-electron transfers to form *NNH, *NNHH, and *NNH_3. Hydrogenation weakens the N≡N bond, enabling eventual dissociation into NH_3. The right portion of Figure 1b portrays the hydrogenation and desorption of the lower N atom to create another N vacancy, completing the cycle. Active and selective ENRR electrocatalysts should readily form N vacancies, adsorb nitrogen species strongly relative to hydrogen, and exhibit favorable kinetics and thermodynamics of successive proton-electron transfers to form the above surface intermediates.

$^{14}N/^{15}N$ isotopic exchange experiments help establish the existence of an MvK mechanism during ENRR by oxynitrides [9]. For example, Figure 2a shows the concentration profiles of ^{14}N and ^{15}N surface sites on a VON surface, where ^{14}N surface sites were exposed first to $^{15}N_2$ gas, inducing turnover to incorporate ^{15}N from the reagent. At times after the vertical dashed line, the surface is exposed to $^{14}N_2$ gas, partially reversing the turnover and showing that lattice nitrogen in VON participates in an MvK mechanism [9].

The challenge of tuning N_2 and H_2 adsorption energies represents an exciting opportunity for perovskite and other complex oxynitrides. Many metals and alloys have poor selectivity for ENRR over HER because they adsorb H_2 too strongly. Adsorbate scaling relations on these materials limit *N or *N_2 coverages, hindering ENRR activity [7]. However, oxynitride electrocatalysts may break these scaling relationships to favor higher *N_2 coverages at low overpotentials. For example, Figure 2b shows how N vacancies on VON surfaces of different bulk O concentrations are preferentially filled by *N_2 over *O, *OH, or *H. Figure 2c shows that after N fills a vacancy site on VON, H prefers to adsorb to this surface N site even if adjacent V sites are available regardless of bulk oxygen composition, encouraging hydrogenation of *N to NH_3 rather than saturation of V sites. Computed ENRR reaction energy profiles show that while intermediates bind stronger to O vacancies than to N vacancies, overall reaction kinetics are more favorable when intermediates bind to N vacancies [9]. These insights both support the MvK mechanism and rationalize the hypothesis that surface N vacancies are the active ENRR sites. Complex oxynitrides, including perovskite oxynitrides with two or more metal cations, may possess these desirable properties but with much higher tunability.

More studies are needed around perovskite oxynitrides' ability to form surface N vacancies under electrochemical conditions. A tradeoff exists between ease of N vacancy formation and higher energy of the defected surface, which increases adsorption strength of N_2 [10]. In perovskite oxides, the oxygen *p*-band center is an electronic structure descriptor of the

metal-oxygen bond strength [11]. A higher oxygen *p*-band center corresponds to less ionic charge transfer from the metal cations to oxygen, weakening metal-oxygen bonds and facilitating formation of O vacancies. A similar correlation between the nitrogen *p*-band center and metal-nitrogen bond strength may exist for perovskite oxynitrides, such that the N *p*-band center is a descriptor for both N vacancy formation energy and for $*N_2$ adsorption strength. Future studies should examine the dependence of the N *p*-band center on perovskite cations and anion ordering in the lattice, as well as combinations of geometric and electronic properties that might more fully describe ENRR on these materials. Linking the electronic structure to geometry will lead to useful design rules for creating active and selective ENRR electrocatalysts.

Materials informatics approaches can elucidate trends and identify descriptors across the space of perovskite oxynitrides, using databases such as Materials Project, AFLOW, JARVIS, and NOMAD repositories. Importantly, such studies should also evaluate the thermodynamic stability and possible surface reconstruction of candidate materials under electrochemical conditions. Computational Pourbaix diagrams at the relevant pH and potential ranges and quantum mechanical calculations can help guide experimental work [12].

When studying perovskite oxynitrides for ENRR, multiple approaches should be used to experimentally verify NH_3 production [1]. This quantification often uses ion chromatography coupled with mass spectrometry, or frequency-selective nuclear magnetic resonance mass spectrometry. However, these approaches are prone to interference from background H_3O^+, H_2O, and NH_3 and are time-consuming [10]. A liquid chromatography method based on the reaction of dansyl chloride with NH_3 product promises to resolve ^{15}N from ^{14}N quickly and without background interference [13]. Carefully designed ^{15}N isotope studies are critical to verify that produced NH_3 arises principally from N_2 reagent and not from leached lattice N [14].

In summary, multi-metal complex oxynitrides, including perovskite oxynitrides, represent an exciting and underexplored class of potential ENRR electrocatalysts. Due to the wide range of possible perovskite oxynitride compositions, the field would benefit from design principles to predict active and stable catalysts. Future data-driven studies may identify activity or stability descriptors to accelerate the discovery of improved catalysts for ENRR. Exploring the vast underlying materials space and formulating design rules can also lead to new strategies based on doping, interfacial strain, ferroelectric polarization, and magnetization, which can be used to favorably alter kinetics for other electrochemical and thermochemical reactions.

Acknowledgments
This work was supported, in part, by the U.S. Department of Energy through the Los Alamos National Laboratory. Los Alamos National Laboratory is operated by Triad National Security, LLC, for the National Nuclear Security Administration of the U.S. Department of Energy (contract no. 89233218CNA000001). Funding for this work was provided by the Laboratory

Directed Research and Development program of Los Alamos National Laboratory under project no. 20200294ER and by startup funds of Goldsmith provided by the University of Michigan.

References

1. Foster, S.L., Bakovic, S.I.P., Duda, R.D., Maheshwari, S., Milton, R.D., Minteer, S.D., Janik, M.J., Renner, J.N., and Greenlee, L.F. (2018). Catalysts for nitrogen reduction to ammonia. Nat. Catal. *1*, 490–500.

2. Ceballos, B.M., Pilania, G., Ramaiyan, K.P., Banerjee, A., Kreller, C., and Mukundan, R. (2021). Roads less traveled: nitrogen reduction reaction catalyst design strategies for improved selectivity. Curr. Opin. Electrochem. *28*, 100723.

3. Wang, M., Liu, S., Qian, T., Liu, J., Zhou, J., Ji, H., Xiong, J., Zhong, J., and Yan, C. (2019). Over 56.55% Faradaic efficiency of ambient ammonia synthesis enabled by positively shifting the reaction potential. Nat. Commun. *10*, 341.

4. Wang, H.-C., Schmidt, J., Botti, S., and L. Marques, M.A. (2021). A high-throughput study of oxynitride, oxyfluoride and nitrofluoride perovskites. J. Mater. Chem. A *9*, 8501–8513.

5. Ologunagba, D., and Kattel, S. (2021). Transition metal oxynitride catalysts for electrochemical reduction of nitrogen to ammonia. Mater. Adv. *2*, 1263–1270.

6. Pan, J., Hansen, H.A., and Vegge, T. (2020). Vanadium oxynitrides as stable catalysts for electrochemical reduction of nitrogen to ammonia: the role of oxygen. J. Mater. Chem. A *8*, 24098–24107.

7. Yang, X., Nash, J., Anibal, J., Dunwell, M., Kattel, S., Stavitski, E., Attenkofer, K., Chen, J.G., Yan, Y., and Xu, B. (2018). Mechanistic insights into electrochemical nitrogen reduction reaction on vanadium nitride nanoparticles. J. Am. Chem. Soc. *140*, 13387–13391.

8. Zeinalipour-Yazdi, C.D., Hargreaves, J.S.J., and Catlow, C.R.A. (2015). Nitrogen activation in a Mars–Van Krevelen mechanism for ammonia synthesis on CO_3Mo_3N. J. Phys. Chem. C *119*, 28368–28376.

9. Yang, X., Kattel, S., Nash, J., Chang, X., Lee, J.H., Yan, Y., Chen, J.G., and Xu, B. (2019). Quantification of active sites and elucidation of the reaction mechanism of the electrochemical nitrogen reduction reaction on vanadium nitride. Angew. Chem. Int. Ed. *58*, 13768–13772.

10. Qiao, Z., Johnson, D., and Djire, A. (2021). Challenges and opportunities for nitrogen reduction to ammonia on transitional metal nitrides via Mars-van Krevelen mechanism. Cell Rep. Phys. Sci. *2*, 100438.

11. Hwang, J., Rao, R.R., Giordano, L., Katayama, Y., Yu, Y., and Shao-Horn, Y. (2017). Perovskites in catalysis and electrocatalysis. Science *358*, 751–756.

12. Wang, Z., Zheng, Y.-R., Chorkendorff, I., and Nørskov, J.K. (2020). Acid-stable oxides for oxygen electrocatalysis. ACS Energy Lett. *5*, 2905–2908.

13. Yu, W., Lewis, N.S., Gray, H.B., and Dalleska, N.F. (2020). Isotopically selective quantification by UPLC-MS of aqueous ammonia at submicromolar concentrations using dansyl chloride derivatization. ACS Energy Lett. *5*, 1532–1536.

14. Du, H.-L., Gengenbach, T.R., Hodgetts, R., MacFarlane, D.R., and Simonov, A.N. (2019). Critical assessment of the electrocatalytic activity of vanadium and niobium nitrides toward dinitrogen reduction to ammonia. ACS Sustain. Chem. Eng. *7*, 6839–6850.

Figure Captions.

Figure 1. Overview of the electrocatalytic nitrogen reduction reaction (ENRR) on an $ABON_2$ perovskite oxynitride. (a) Bulk unit cell of an $ABON_2$ perovskite oxynitride. **(b)** Illustration of an associative distal Mars-van-Krevelen mechanism, with N vacancies (N_{vac}, ●) facilitating associative adsorption and stepwise hydrogenation of N_2 to NH_3 Atom key: light blue = N, red = O, green = A, dark blue = B, gray = H.

Figure 2. Experimental and computational investigations of VON. (a) Isotopic exchange experiment showing turnover of ^{14}N sites on VON surface with ^{15}N and the reverse process as a function of time. (b) Adsorption free energies of $*N_2$ on VON surfaces relative to those of *O, *OH, and *H adsorbates, as a function of bulk O concentration. (c) Adsorption energies of H at a surface N site (ΔE_{NH}) relative to adsorption of H at a surface V site (ΔE_{VH}), as a function of bulk O concentration. Panel (a) adapted with permission from [7]. Panels (b) and (c) adapted with permission from [6].

Figures.

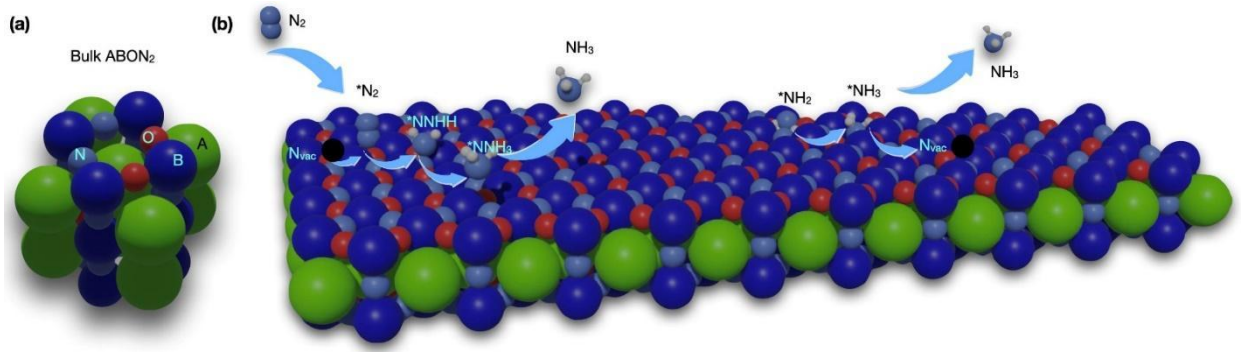

Figure 1.

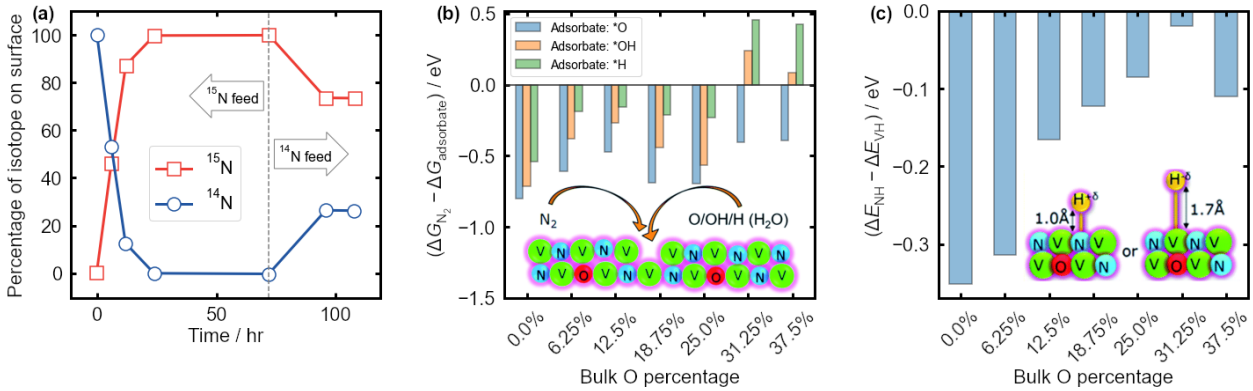

Figure 2.